A R C H I V E S O F M E T A L L U R G Y A N D M A T E R I A L S
Volume 53 2008 Issue 1

P. MIETNIOWSKI*, J. KANAK*, W. POWROŹNIK*, T. STOBIECKI*, P. MAJ**, P. GRYBOŚ**

# APPLICATION OF SILICON STRIP DETECTOR FOR X-RAY DIFFRACTION ON METALLIC MULTILAYERS

# ZASTOSOWANIE KRZEMOWEGO DETEKTORA PASKOWEGO DO BADAŃ DYFRAKCYJNYCH METALICZNYCH UKŁADÓW WIELOWARSTWOWYCH

This paper presents silicon strip detector designed at AGH with front-end electronics based on ASIC (Application Specific Intergraded Circuits) which is used for diffraction measurements of thin films. Application of this detector for diffraction, in comparison to the standard proportional counter, allows to reduce time of measurement up to 100 times. Two types of 128-strip detectors with pitch between strips centers of 75 μm and 100 μm were tested. Angular resolution was determined from measurements of powder standard reference material (SRM 660) $LaB_6$. It was demonstrated that detector with strip pitch 75 μm had better angular resolution than that of 100 μm one. The XRD measurements were performed on the metallic polycrystalline multilayers deposited by sputtering technique: Si(100)/$SiO_2$ 47 nm/*buffer*/IrMn 12 nm/CoFe 15 nm/Al-O 1.4 nm/NiFe 3 nm/Ta 5 nm and Si(100)/$SiO_2$ 500 nm/*buffer*/[Pt 2 nm/Co 0.5 nm]×5. The samples were prepared with four different buffers in order to obtain different texture degree (in the brackets buffers for Pt/Co multilayers): (a) Cu 25 nm, (Cu 10 nm) (b) Ta 5 nm/Cu 25 nm, (Ta 5 nm/Cu 10 nm) (c) Ta 5 nm/Cu 25 nm/Ta 5 nm/Cu 5 nm, (Ta 5 nm/Cu 10 nm/Ta 5 nm) and (d) Ta 5 nm/Cu 25 nm/Ta 5 nm /NiFe 2 nm/Cu 5 nm, (Ta 5 nm/Cu 10 nm/Ta 5 nm/Cu 10 nm). The results measured by our strip detector, conventional proportional counter and commercial X'Celerator detector are similar in all details specific for diffraction of multilayer. Some advantages of the strip detectors usage for structural analysis of thin films are discussed.

*Keywords*: strip detector of X-ray diffractometer, X-ray diffraction, multilayers, texture
PACS: 07.85. Jy, 61.05. cp, 78.67. Pt, 68.55. jm

Krzemowe detektory paskowe zintegrowane z elektroniką "front-end" zaprojektowane na AGH w oparciu o układ ASIC (Application Specific Intergraded Circuits) zostały wykorzystane do detekcji promieniowania rentgenowskiego w eksperymentach dyfrakcyjnych układów cienkowarstwowych. Zastosowanie tych detektorów w porównaniu z licznikami proporcjonalnymi pozwala zredukować czas pomiaru do około 100 razy. Przetestowano dwa typy detektorów 128-paskowych o odległościach pomiędzy paskami 75 μm i 100 μm. Pomiary kątowej zdolności rozdzielczej wykonane na próbkach proszkowych $LaB_6$, pokazały, że detektor z odległością pomiędzy paskami 75 μm posiada lepszą zdolność rozdzielczą. Przeprowadzono pomiary dyfrakcyjne na wybranych układach cienkowarstwowych naniesionych techniką jonowego rozpylenia. Układy te miały następującą budowę: podłoże Si(100)/$SiO_2$ 47 nm/*warstwy buforowe* /IrMn 12 nm/CoFe 15 nm/Al-O 1.4 nm/NiFe 3 nm/Ta 5 nm oraz Si(100)/$SiO_2$ 500 nm/*warstwy buforowe*/[Pt 2 nm/Co 0.5 nm]×5. Jako warstwy buforowe zastosowano następujące układy wielowarstwowe (w nawiasach warstwy buforowe dla układów wielowarstwowych Pt/Co): (a) Cu 25 nm, (Cu 10 nm) (b) Ta 5 nm/Cu 25 nm, (Ta 5 nm/Cu 10 nm) (c) Ta 5 nm/Cu 25 nm/Ta 5 nm/Cu 5 nm, (Ta 5 nm/Cu 10 nm/Ta 5 nm) and (d) Ta 5 nm/Cu 25 nm/Ta 5 nm /NiFe 2 nm/Cu 5 nm, (Ta 5 nm/Cu 10 nm/Ta 5 nm/Cu 10 nm). Otrzymano podobne wyniki zarówno przy wykorzystaniu licznika proporcjonalnego, detektora paskowego jak i komercyjnego detektora X'Celerator. Przedyskutowano zalety krzemowego detektora paskowego w zastosowaniu do badań dyfrakcyjnych układów cienkowarstwowych.

## 1. Introduction

The silicon strip detectors are widely used in particle physics experiments [1] as well as in X-ray diffraction [2-5] using one-dimensional (1-D) position sensitive detection technique. Several strip detectors like X'Celerator (PANalytical) [6], LynxEye (Bruker) [7] and D/tex Ultra (Rigaku) [8] are available commercially. These detectors are a new generation ones for higher speed and higher resolution of X-Ray Diffraction (XRD) measurements than traditional proportional counters. They are cost-effective 1-D detectors for measuring a wide angular range simultaneously, thereby significantly reducing measurement time in comparison with point detectors (e.g. proportional counters), while achieving high resolution and excellent peak shape.

* DEPARTMENT OF ELECTRONICS, AGH UNIVERSITY OF SCIENCE AND TECHNOLOGY, 30-059 KRAKÓW, 30 MICKIEWICZA AV., POLAND
** DEPARTMENT OF MEASUREMENT AND INSTRUMENTATION, AGH UNIVERSITY OF SCIENCE AND TECHNOLOGY, 30-059 KRAKÓW, 30 MICKIEWICZA AV., POLAND

In our studies we use the strip detector with integrated front-end electronics based on ASIC (Application Specific Intergraded Circuits) designed at AGH by Gryboś and his coworkers [9]. This system is characterized by high homogeneity and high efficiency of detecting channels.

For the first time to our knowledge, we demonstrate application of strip detectors, for X-ray diffraction measurements: θ-2θ-scan and ω-scan for metallic multilayers.

The paper is organized as follows. Section 2 describes arrangement of diffraction experiment, detector and details of samples fabrication. The measurement results and their analysis for different magnetic multilayer systems are discussed in Section 3. Finally, the paper is summarized by conclusions.

## 2. Experimental

The strip detectors were mounted on the goniometer arm of Philips X'Pert diffractometer. Experiments were performed using Ni-filtered Cu radiation. Angular resolution has been measured on the powder standard reference material (SRM 660) $LaB_6$ for the strip detectors with strip pitch 75 μm and 100 μm as well as for the proportional counter, in Bragg-Brentano geometry. Diffraction measurements (θ-2θ-scan and ω-scan) of multilayers were performed by means of our strip detector, conventional proportional counter and for selected samples on X'Celerator.

### 2.1. Detector

The sensor was made of highly resistive silicon segmented into 128 reverse-biased diodes. The signal from the strips was read by two 64-channels ASIC (called DEDIX Dual Energy Digital X-ray Imaging) which contain binary readout architecture and two voltage discriminators per channel. Binary information can easily be stored in an integrated circuit, which allows one to cope with the high intensity of X-ray radiation as each channel works independently. The significant reduction of the measurement time was achieved by:

- high number of strips in silicon detectors (in most cases from tens to hundreds strips),
- small distance between the strips (pitch is mostly in the range from 50 μm to 100 μm),
- high counting rate performance of single electronic readout channel (up to 1 MHz).

The block diagram for a single channel is shown in Fig. 1. Each channel is built of a charge sensitive amplifier (CSA) with a pole-zero cancellation circuit, a shaper CR-$RC^2$ with a peaking time of 160 ns, two independent discriminators and two independent 20-bit counters [9]. The size of the input device in CSA has been optimized for a detector capacitance in the range of 1-3 pF per strip. The ASIC is designed in 0.35 μm CMOS process and its total area is 3900×5000 $\mu m^2$. The DEDIX has a binary readout architecture. DEDIX IC contains a command decoder, DACs (Digital Analog Converter) and calibration circuits, which increase the functionality and testability of the IC. Because of the additional 7-bit correction DAC in each channel, there is a possibility to precisely tune the DC level at the discriminator inputs. Internal correction DAC implemented in each channel independently ensures the low spread of effective threshold of discriminators at 0.4 mV on one-sigma level.

The mean gain in the multichannel ASIC is 54 μV/el, with good uniformity from channel to channel. The ASIC works with silicon strip detector with strip pitch 75 μm and 100 μm. More details about design of electronics and properties of 64 channel readout ASIC called DEDIX were presented in the paper [9].

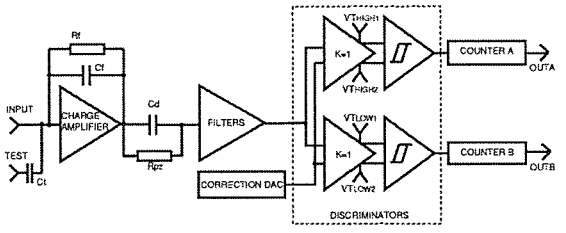


Fig. 1. Block diagram of a single detection channel [9]

### 2.2. The samples

#### 2.2.1. Spin-Valve Magnetic Tunnel Junctions (SV-MTJs)

The typical spin-valve magnetic tunnel junction (SV-MTJ, Fig. 2) is composed of the system of seed-buffer metal layers, then the system of magnetic layers: antiferromagnetic (AF), pinned ferromagnetic (FP) layer (bottom electrode), insulating barrier, ferromagnetic free (FF) layer (top electrode) and the system of metal protection layers. This multilayers system is a fundamental unit of M-RAM cells (Magnetic Random Access Memory) or read head of hard disc drive. During MTJ fabrication, such as M-RAM or read head elements, that are grown by sputtering deposition, the metal layers are typically polycrystalline and tend to grow in a columnar-like fashion [10].

The spin valve magnetic tunnel junctions with the layers stack (Fig. 2): substrate/buffers (*a*, *b*, *c* and *d*)/IrMn 12 nm/CoFe 15 nm/Al-O 1.4 nm/NiFe 3 nm/Ta 5 nm were deposited by dc magnetron sputtering on-

to thermally oxidized ($SiO_2$ 47 nm) (100)Si wafer (the details about preparation are published elsewhere [11, 12]). Four different systems of buffer layers have been investigated: (a) Cu 25 nm, (b) Ta 5 nm/Cu 25 nm, (c) Ta 5 nm/Cu 25 nm/Ta 5 nm/Cu 5 nm and (d) Ta 5 nm/Cu 25 nm/Ta 5 nm/NiFe 2 nm/Cu 5 nm, in order to check the texture of IrMn and CoFe layers induced by buffer layers.

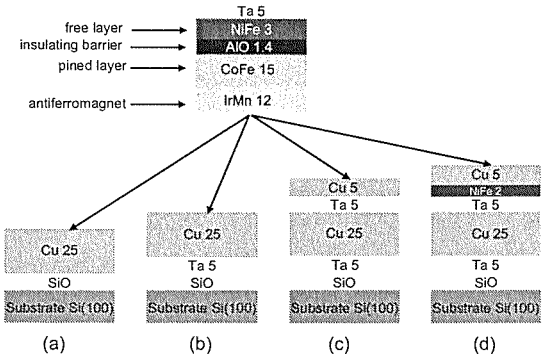


Fig. 2. The stacks of SV-MTJ layers with buffers: (a) Cu, (b) Ta/Cu, (c) Ta/Cu/Ta/Cu and (d) Ta/Cu/Ta/NiFe/Cu. The thickness of the particular sublayer is given in nanometers

### 2.2.2. Pt/Co periodic systems

The stack of [Pt 2 nm/ Co 0.5 nm]×5/ Pt 2 nm multilayers (Fig. 3) were grown on four different seed-buffers: (A) Cu 10 nm, (B) Ta 5 nm/Cu 10 nm, (C) Ta 5 nm/Cu 10 nm /Ta 5 nm, and (D) Ta 5 nm/Cu 10 nm /Ta 5 nm/Cu 10 nm. Buffers and stacks of [Pt/Co] were deposited by dc magnetron sputtering at room temperature on 500 nm thick $SiO_2$ of Si(100) wafer (preparation details are published elsewhere [13]). Such multilayers are characterized by perpendicular to the film plane magnetic anisotropy, which is determined by the texture degree of buffer layers [13, 14]. The perpendicular anisotropy is a very important parameter for application Pt/Co multilayers in high density recording media [15].

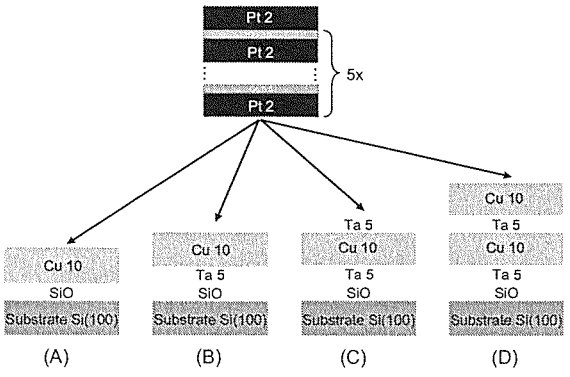


Fig. 3. The stacks of Pt/Co multilayer with buffers: (A) Cu, (B) Ta /Cu, (C) Ta/Cu/Ta and (D) Ta/Cu/Ta/Cu. The thickness of the particular sublayers is given in nanometers

## 3. Results and Discussion

### 3.1. Angular resolution

Angular resolution has been measured on the standard reference material (SRM 660) $LaB_6$ for the strip detectors with strip pitch 75 μm and 100 μm and for the proportional counter. The comparison of angular resolution for both detectors as well as for classical proportional counter is shown in Fig. 4. Obtained data are very close to the measurements with proportional counter, however, for detector with 75 μm strip pitch the angular resolution is about 10% better than for detector with 100 μm strip pitch. The detector with 75 μm strip pitch was used for measurements of multilayers.

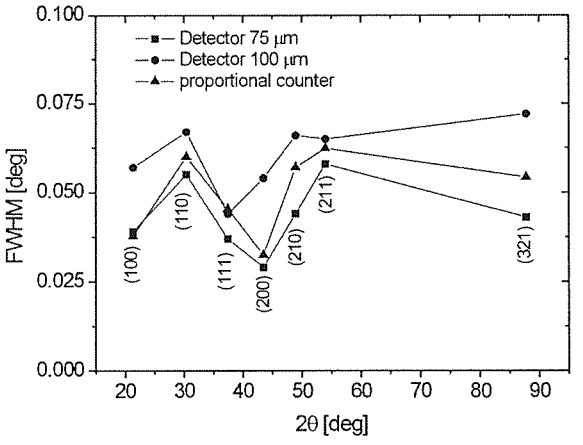


Fig. 4. Comparison of FWHM determined from $LaB_6$ reference sample for detectors with 75 μm and 100 μm strip pitch and proportional counter

### 3.2. Strip detector in reciprocal space

In this section 1-D detector's path in the reciprocal space will be explained and details of the measurements on weak and strong textured multilayers will be discussed. In the left diagram (Fig. 5a) scans and corresponding profiles on poorly textured sample (SV-MTJ-a, where diffraction peaks are very broad) have been measured in 2θ steps equal to the whole angular range (2.43°) of 75 μm strip detector. In this case only three steps of measurements are enough to cover the considered 2θ angle range. However, in the case of strongly textured sample (SV-MTJ-b, Fig. 5b), when diffraction peaks are narrow, measurements have been performed in 2θ steps much smaller than the angle range of strip detector, in order to exactly cover specular range of θ-2θ measurements. For that reason the range of 2θ step should be always, in diffraction experiments described in this paper, properly adjusted to the texture degree of the investigated sample.

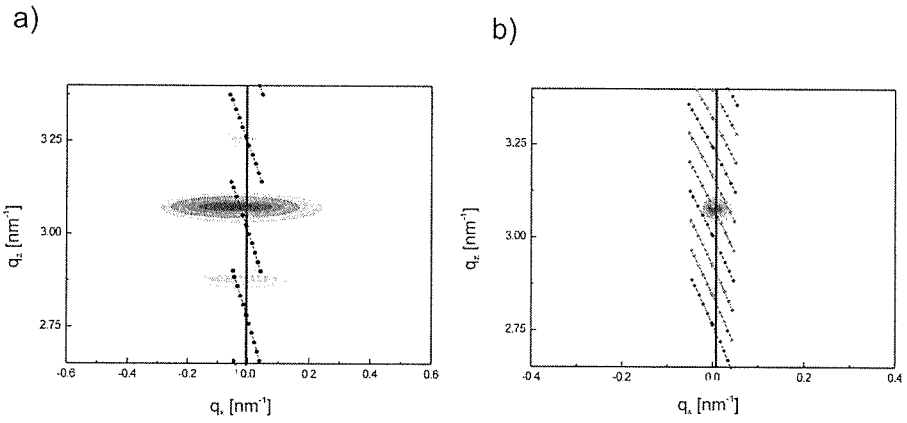


Fig. 5. Strip detector measurements in reciprocal space on poorly textured sample (SV-MTJ-a) a) and strongly textured sample (SV-MTJ-b) b) The vertical line (for $q_x = 0$) represents θ-2θ scan for point detector (proportional counter)

### 3.3. Measurements of Multilayers

#### 3.3.1. SV-MTJs

Measurements of θ-2θ-scans and ω-scans were performed for SV-MTJ grown on different buffers. Diffraction patterns of SV-MTJ multilayer with buffer system (b) in wide angle range, measured by proportional counter and strip detector are shown in Fig. 6a. Only diffraction peaks from cubic crystal planes fcc-Cu(111), fcc-IrMn(111) and bcc-CoFe(110) of the first and second order and peaks from Si single crystal substrate are observed. The circles corresponds to the results for proportional counter. It is worth noticing that in this case the total measurement time was 16 hours. The solid line corresponds to strip detector and measurement time for the group of the first order (111) peaks was only 30 minutes and for the group of the second order (222) peaks was about 50 minutes. The profiles of θ-2θ for samples with buffer Cu (a), Ta/Cu (b), Ta/Cu/Ta/Cu (c) and Ta/Cu/Ta/NiFe/Cu (d) measured with 2θ step 0.2° are shown in Fig. 6b.

The intensities of the IrMn(111), Cu(111) and CoFe(110) peaks are higher by about two orders of magnitude in the case of samples with buffer (b) than for that with buffer (a). It indicates very strong (111) texture of the sample with buffer (b). For the (a) buffer small intensity peak of Cu(200) was observed in addition to dominating Cu(111) peak. The existence of both crystallographic orientations indicates more disordered structure of single Cu layer (system (a)) than Ta/Cu bilayer (b). The intermediate texture degree is specific for multilayers with buffers (c) and (d).

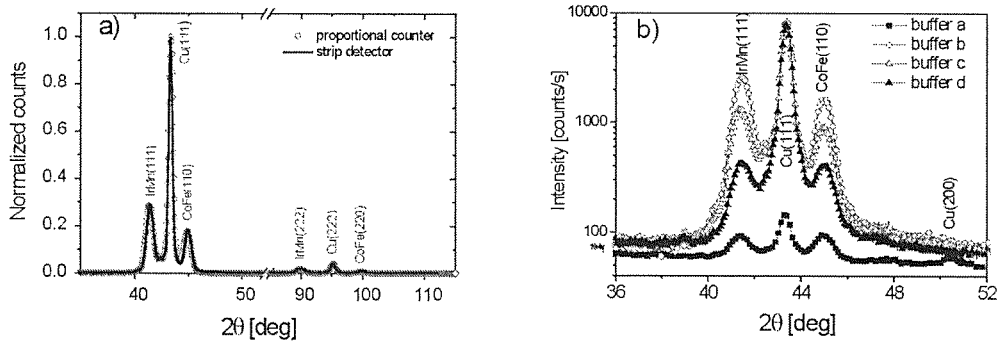


Fig. 6. Normalized θ-2θ scans of SV-MTJ Si(100)/$SiO_2$ 47 nm/buffers (*a*, *b*, *c* and *d*)/IrMn 12 nm/CoFe 15 nm/Al-O 1.4 nm/NiFe 3 nm/Ta 5 nm with buffer Ta 5 nm/Cu 25 nm (b) measured by the proportional counter (circles) and by the strip detector (solid line) with 75 μm pitch a). θ-2θ scans of SV-MTJs: square – buffer Cu 25 nm (a), circle – buffer Ta 5 nm/Cu 25 nm (b), open triangle – buffer Ta 5 nm/Cu 25 nm/Ta 5 nm/Cu 5 nm (c) and filled triangle – buffer Ta 5 nm/Cu 25 nm/Ta 5 nm/NiFe 2 nm/Cu 5 nm (d) b). The measurements were performed with 2θ step 0.2°

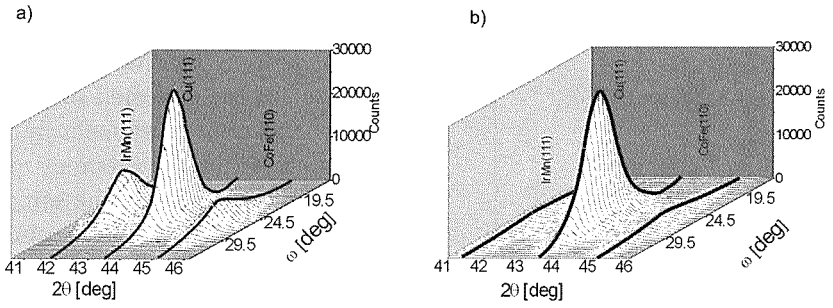


Fig. 7. Three-dimensional diagram for SV-MTJ with strong texture – buffer Ta 5 nm/Cu 25 nm a), for sample with poor texture – buffer Cu 25 nm b)

TABLE 1

The standard deviation of Gaussian distribution $2\sigma$ values of rocking curve profiles of Cu(111), IrMn(111), and CoFe(110) fo · SV-MTJs with (a), (b), (c) and (d) buffers, measured by strip detector and proportional counter

| Buffer | Cu(111) | | IrMn(111) | | CoFe(110) | |
|---|---|---|---|---|---|---|
| | Proportional $2\sigma$ [°] | Strip $2\sigma$ [°] | Proportional $2\sigma$ [°] | Strip $2\sigma$ [°] | Proportional $2\sigma$ [°] | Strip $2\sigma$ [°] |
| (a) | 11.7±0.2 | 13.3±0.6 | 15.6±0.4 | 17.8±0.8 | 14.5±0.3 | 15.7±0.9 |
| (b) | 2.32±0.01 | 2.29±0.01 | 2.67±0.01 | 2.63±0.02 | 3.06±0.01 | 3.07±0.01 |
| (c) | 2.37±0.01 | 2.38±0.01 | 4.33±0.02 | 4.48±0.03 | 4.66±0.01 | 4.77±0.03 |
| (d) | 2.42±0.01 | 2.42±0.01 | 8.58±0.05 | 8.89±0.09 | 7.48±0.02 | 7.24±0.09 |

In order to determine the degree of texture of the particular sublayers in SV-MTJ with (a), (b), (c) and (d) buffer systems, the rocking curves (ω-scan) were recorded by silicon strip detector with 75 μm pitch. Fig. 7 shown three-dimensional diagram (in coordinates 2θ and ω) for samples with strong (Fig. 7a) and poor texture (Fig. 7b). Corresponding standard deviation of the Gaussian distribution $2\sigma$ values obtained from fitting of the rocking curve profiles recorded by proportional counter and strip detector are collected in Table 1. One can see that the width of rocking curves measured by both detectors are comparable within the error of measurement. Large values of $2\sigma$ and wide distributions of the rocking curves are characteristic for the sample with (a) buffer, while narrow distributions are found for the sample with (b) buffer. It is easy to deduce that single Cu seed-buffer layer (system (a)) is weak (111) textured, while in buffers (b), (c) and (d) its texture is strong. It means that Ta 5 nm thick seed layer, deposited on amorphous oxidized silicon, improves the Cu layer texture and this effect is forwarded to magnetic layers of IrMn and CoFe [11, 12]. Implementation of additional layers between Cu and IrMn (see Fig. 2): Ta 5 nm/Cu 5 nm (in buffer (c)) and Ta 5 nm/NiFe 2 nm/Cu 5 nm (in buffer (d)) gradually weakens the texture of upper layers. More details about crystallographic texture of this samples can be found in the papers of Kanak [11, 12, 14].

### 3.3.2. Periodic multilayers of Pt/Co

The θ-2θ profiles for [Pt 2 nm/ Co 0.5 nm]×5/ Pt 2 nm on buffers: Cu 10 nm (A), Ta 5 nm/Cu 10 nm (B), Ta 5 nm/Cu 10 nm/Ta 5 nm (C), Ta 5 nm/Cu 10 nm/Ta 5 nm/Cu 10 nm (D) are shown in Figure 8. The measurements were performed by the 75 μm pitch strip detector with 2θ step 0.2°. In order to check the (111) texture of Pt/Co, the multilayers were deposited on buffer layers with different texture degree of Cu. The (111) texture of Pt/Co very strong influences the value of perpendicular anisotropy constant of Pt/Co multilayers, which is important for the application of Pt/Co as perpendicular recording media [14, 16].

The highest Pt/Co superlattice peaks are for samples with buffer (D), then (B) and (C). The lowest one is for sample with buffer (A), because Cu single layer (buffer A), deposited on amorphous silicon oxide is weakly textured in [111] direction in comparison with Ta/Cu bilayer (buffer B). It means that Ta 5 nm thick seed layer (deposited on amorphous oxidized silicon) as well as the further repetition Ta/Cu (buffers C and D), improves the (111) Cu texture and this effect is forwarded to magnetic layers of Pt/Co which also improves their (111) texture. Please, note that the repetition by Ta 5 nm/Cu 10 nm bilayers when Cu is two times thicker improves the texture of (111) Cu in contrast to buffers with thin Cu (5 nm).

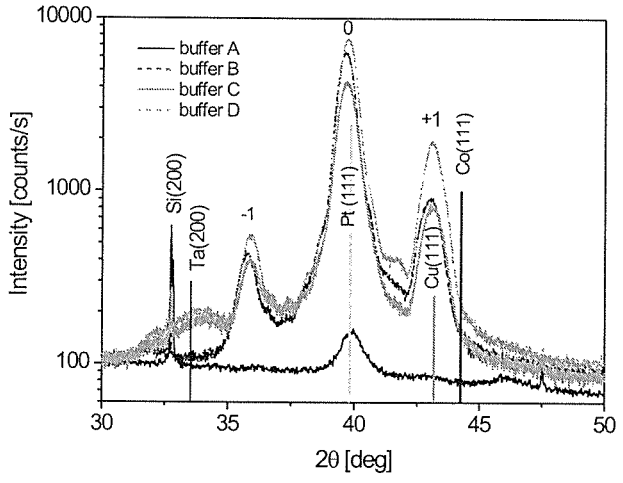


Fig. 8. θ-2θ scans of Si(100)/$SiO_2$ 500 nm/*buffer(A, B, C and D)*/[Pt 2 nm/ Co 0.5 nm]×5/ Pt 2 nm multilayers measured by strip detector with 75 μm pitch. The measurements were performed with 2θ step 0.2°

The comparison of the obtained results is shown in Fig. 9: for sample with buffer B for silicon strip detector (solid line), commercial X'Celerator (dashed line) and proportional counter (dotted line). It is clearly seen that the results for all detectors are very close. It is noteworthy that the measurement time for proportional counter was about 80 minutes, while for our strip detector and X'Celerator was only 6 minutes.

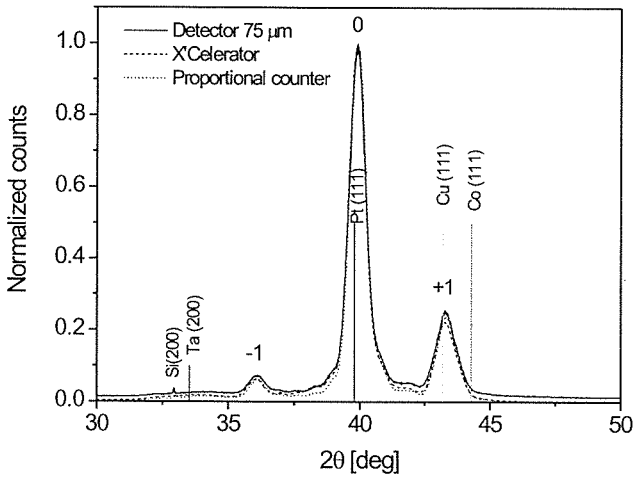


Fig. 9. Comparison of the θ-2θ scans obtained for multilayer with buffer Ta 5 nm/Cu 10 nm (B) for strip detector (solid line), commercial X'Celerator (dashed line) and proportional counter (dotted line)

Rocking curves (ω-scans) for the main (n = 0) peak of superlattice (at position 2θ = 39.9°) were measured using strip detector and obtained results for buffers (B), (C), and (D) are shown in Fig. 10. The standard deviation of Gaussian distribution $2\sigma$ obtained from fitting of these profiles recorded by proportional counter and strip detector are collected in Table 2. One can see that width of rocking curves measured by both detectors are comparable within the accuracy of measurements. In the case of Pt/Co multilayers the sample with buffer (D) has the strongest texture, however similarly to the magnetic tunnel junctions, the weakest texture for the sample with buffer (A) was observed.

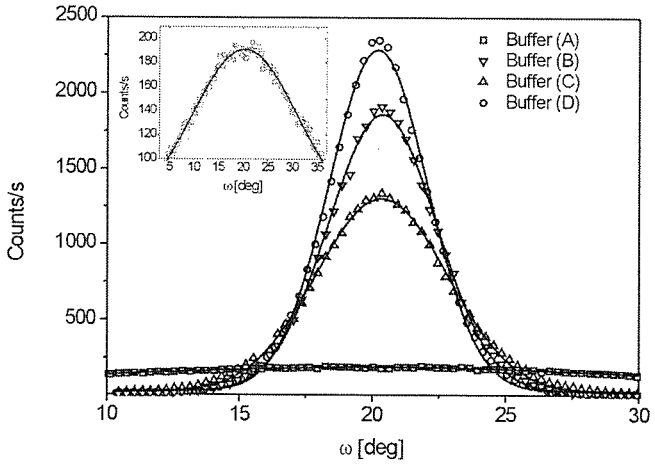


Fig. 10. Rocking curve (ω-scans) recorded on n = 0 superlattice peak of Pt/Co measured by 75 μm strip detector. Solid lines are fittings to the Gaussian distribution. Inset depicts enlargement of ω-scans of (A) buffer

TABLE 2
The standard deviation of Gaussian distribution 2σ values of rocking curve profiles recorded on n = 0 superlattice peak from multilayers of Pt/Co with (A), (B), (C) and (D) buffers, measured by strip detector and proportional counter

| Sample | Proportional counter 2σ [°] | Strip detector 2σ [°] |
|---|---|---|
| Buffer (A) | 21.4±0.7 | 23.8±0.9 |
| Buffer (B) | 4.01±0.02 | 4.03±0.02 |
| Buffer (C) | 4.98±0.02 | 4.91±0.02 |
| Buffer (D) | 3.68±0.01 | 3.69±0.02 |

## 4. Conclusions

From the point of view of the efficiency of the diffraction analysis of thin films and multilayer systems, it is very important to shorten the measurement time. Strip detector allows for a reduction of measurement time up to 100 times. Our silicon strip detector has been used successfully for diffraction of textured multilayers and the obtained results are comparable with data recorded by proportional counter and commercial X'Celerator. We can finally say that diffractometers equipped by strip detectors essentially shorten the measurement time of the

sample with small amount of material as e.g. thin films. The measured, by our strip detector and X'Celerator, θ-2θ and rocking curve scans are similar in all details specific for diffraction of multilayers. This fact confirms high quality of designed silicon strip detector and ASIC electronic circuits.

**Acknowledgements**

This work was supported by Ministry of Science and Higher Education of Poland under grant No. PBZ-MIN012/T11/03.

REFERENCES

[1] Y. Unno, ATLAS silicon Microstrip Semiconductor Tracker (SCT), Nucl. Instr. and Meth. **A453**, 109-120 (2000).

[2] A. Zięba, W. Dąbrowski, P. Gryboś, W. Powroźnik, T. Stobiecki, K. Świentek, J. Słowik, P. Wiącek, Prototype silicon position-sensitive detector working with Bragg-Brentano powder diffractometer, Acta Phys. Polon. **A101**, 629-634 (2002).

[3] A. Zięba, W. Dąbrowski, P. Gryboś, W. Powroźnik, J. Słowik, T. Stobiecki, K. Świentek, P. Wiącek, 128-channel silicon strip detector installed at a powder diffractometer, Mater. Sci. Forum **443-444**, 175-180 (2004).

[4] D. Loukas, V. Psycharis, E. Karvelas, A. Pavlidis, N. Haralabidis, J. Mousa, Powder X-ray diffraction diagram with a silicon microstrip detector, IEEE Trans. Nucl. Sci. **NS-47**, 877-880 (2000).

[5] L. Tarkowski, J. Bonarski, W. Dąbrowski, Application of the Si-strip detector in X-ray crystallographic texture measurements, Nucl. Inst. and Meth. **A551**, 178-182 (2005).

[6] http://www.panalytical.com/.

[7] http://www.bruker-axs.com/.

[8] http://www.rigaku.com/.

[9] P. Gryboś, P. Maj, L. Ramello, K. Świentek, Measurement of matching and high count rate performance of multichannel ASIC for digital X-ray imaging systems, IEEE Trans. Nucl. Sci. **54**, 1207-1215 (2007).

[10] T. Stobiecki, J. Kanak, J. Wrona, M. Czapkiewicz, C. G. Kim, C. O. Kim, M. Tsunoda, M. Takahashi, Correlation between structure and exchange coupling parameters of IrMn based MTJ, Phys. Stat. Sol. (a) **201**, 1621-1627 (2004).

[11] P. Wiśniowski, T. Stobiecki, J. Kanak, G. Reiss, H. Brückl, Influence of buffer layer texture on magnetic and electrical properties of IrMn spin valve magnetic tunnel junctions, J. Appl. Phys. **100**, 013906 (2006).

[12] J. Kanak, X-ray diffraction on multilayers systems-methods of measurement and models, PhD thesis, AGH Kraków 2006.

[13] J. Kanak, T. Stobiecki, S. van Dijken, Influence of interface roughness, film texture, and magnetic anisotropy on exchange bias in $[Pt/Co]_3$/IrMn and IrMn/$[Co/Pt]_3$ multilayers, accepted for publication in IEEE Transactions on Magnetics.

[14] J. Kanak, M. Czapkiewicz, T. Stobiecki, M. Kachel, I. Sveklo, A. Maziewski, S. van Dijken, Influence of buffer layers on the texture and magnetic properties of Co/Pt multilayers with perpendicular anisotropy, Phys. Stat. Sol. (a) **204**, 3950-3953 (2007).

[15] S. Khizroev, D. Litvinov, Perpendicular Magnetic Recording (Kluwer Academic Publishers, 2004).

[16] S. van Dijken, M. Crofton, J. M. D. Coey, M. Czapkiewicz, M. Zoladz, T. Stobiecki, Magnetization reversal and field annealing effects in perpendicular exchange-biased Co/Pt multilayers and spin valves with perpendicular magnetization, J. Appl. Phys. **99**, 083901 (2006).

*Received: 3 December 2007.*